Constraints on the Topology of the Universe: Extension to General Geometries

Pascal M. Vaudrevange,[1,2] Glenn D. Starkman,[3] Neil J. Cornish,[4] and David N. Spergel[5]

[1]*DESY, Notkestrasse 85, 22607 Hamburg, Germany*
[2]*CERCA & Department of Physics, Case Western Reserve University, 10900 Euclid Ave, Cleveland, OH 44106, USA*
[3]*CERCA, ISO & Department of Physics, Case Western Reserve University, 10900 Euclid Ave, Cleveland, OH 44106, USA*
[4]*Department of Physics, Montana State University, Bozeman, Montana 59717, USA*
[5]*Department of Astrophysical Sciences, Princeton University, Princeton, New Jersey 08544, USA*
(Dated: June 15, 2012)

We present an update to the search for a non-trivial topology of the universe by searching for matching circle pairs in the cosmic microwave background [1] using the WMAP 7 year data release. We extend the exisiting bounds to encompass a wider range of possible topologies by searching for matching circle pairs with opening angles $10° \leq \alpha \leq 90°$ and separation angles $11° \leq \theta \leq 180°$. The extended search reveal two small anomalous regions in the CMB sky. Numerous pairs of well-matched circles are found where both circles pass through one or the other of those regions. As this is not the signature of any known manifold, but is a likely consequence of contamination in those sky regions, we repeat the search excluding circle pairs where both pass through either of the two regions. We then find no statistically significant pairs of matched circles, and so no hints of a non-trivial topology. The absence of matched circles increases the lower limit on the length of the shortest closed null geodesic that self-intersects at our location in the universe (equivalently the injectivity radius at our location) to 98.5% of the diameter of the last scattering surface or approximately 26Gpc. It extends the limit to any manifolds in which the intersecting arcs of said geodesic form an angle greater than $10°$.

I. INTRODUCTION

The search for a non-trivial topology of the universe has enjoyed a long and fascinating history. Using different methods – from searching for specific topologies to the more general circles in the sky approach [2] – the cosmic microwave background (CMB) has been analyzed extensively, looking for any signs that light from the same object reaches us by more than one path (see [3] for a review of the various suggested methods, including [1, 2, 4–22]). So far, all specialized efforts to detect specific topologies as well as the search for matching opposing circles in the sky have failed to detect any sign of a non-trivial topology of our universe.

The circles-in-the-sky method, which we adopt in this paper, is based on the following intuitive picture. For illustrative purposes, assume that the true topology of the universe is a 3-torus, with unit cell size smaller than the Hubble horizon (see Figure 1). This can be thought of as a tiling of flat space by identical cubes. An observer, such as ourselves, performing a series of cosmic microwave background (CMB) observations somewhere in one of the cubes, has clones identically located in each of the other cubes performing the identical series of observations. Centered around the observer is the 2-sphere of the surface of last scattering at $z \approx 1100$, with CMB fluctuations imprinted on it. Around the clone of the observer on the right, there is another 2-sphere of the surface of last scattering. The intersection of both 2-spheres is given by a circle. Both observers will look at the same ring of temperature fluctuations – albeit from different "sides". Both observers are in fact identical, so an observer will see a matching pair of circles: one to the left and to the right. Hence, comparing temperature fluctuations along circles potentially yields information about the topology of our universe. Going away from toroidal geometries, it becomes immediately clear that the separation angle θ (the angle between the centers of the pair of matching circles) need not be $180°$. Also, depending on the orientability or non-orientability of the manifold, circle pairs might have matching temperature fluctuations either both going clockwise around the circles (non-orientable) or one going clockwise and the other anti-clockwise (orientable).

So far, the search for matching anti-podal circles, i.e. circles with separation angles $180°$, or nearly anti-podal circles [1], like other topology searches, has only yielded lower limits on the size of the Universe, and then only for "nearly flat" topologies.

In this work, we apply the circles-in-the-sky statistics to searches for circles pairs of all opening angles $10° \leq \alpha \leq 90°$, and integer separation angles $11° \leq \theta \leq 180°$ with both orientations. This extends the previous searches [1, 6] to cover almost all possible topologies. We find what seems to be a systematic effect at two special positions in the sky that produces spurious signals for osculating circles. Otherwise, we see no evidence of non-trivial topology.

II. METHODOLOGY

As already outlined in the introduction, the most intuitive way to search for a non-trivial topology of the universe is by looking for matching pairs of circular temperature fluctuation patterns in the CMB.

In order to determine the underlying topology of the universe, one would need to scan the full CMB map –
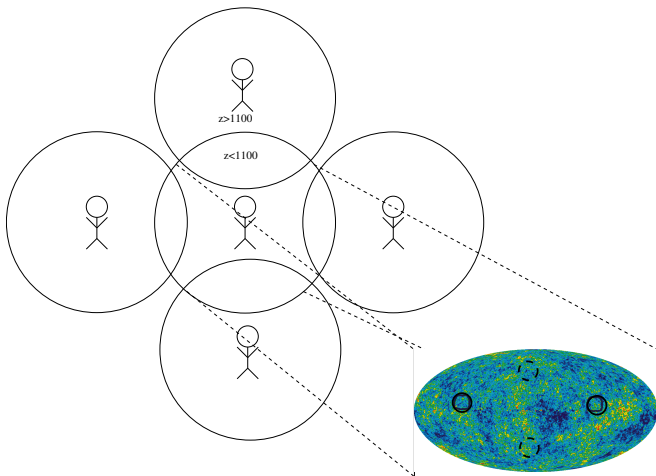
FIG. 1: Schematic geometry of the circles-in-the-sky method. If the topology of the universe is a torus, the observer, located at the center of the 2-sphere of the surface of last scattering, sees matching circles of temperature fluctuations on opposite sides of the CMB sky.

at a Healpix[1] resolution of $N_{\text{side}} = 512$ corresponding to 3×10^6 pixels – for matching circle pairs. To conduct a search for all topologies, i.e. over all opening angles of the circles and all possible separation angles, an enormous number of circle pairs would need to be analyzed. Previously reported searches focussed on nearly flat geometries, where matching circle pairs are at almost opposite positions on the sky, i.e. $\sim 180°$ apart (see [1, 6]).

Thanks to increasing computing power, we can now take a more general approach. In order to obtain an acceptable time frame for completing this project, we superimposed a search grid of $N_{\text{side}} = 128$ onto the map, resulting in 2×10^{10} circle pairs that need to be compared. We compute the goodness of the match for a given circle pair on the full resolution, $N_{\text{side}} = 512$, map. Using a resolution of 512 pixels along a given circle costs about 10^4 operations per compared pair, leading to a total number of operations of 2×10^{14} per opening angle. On a 3GHz CPU, this takes about 20 hours for a single opening angle. Scanning over 200 opening angles corresponds to 4000 CPU hours, easily feasible on modern computer clusters.

Thus we search for all possible topologies, albeit on a somewhat lower resolution grid. Note that we need to run the search twice, once for orientable manifolds and once for non-orientable manifolds, i.e. once for circle pairs that are oppositely oriented, and once for circle pairs that are oriented in the same way.

A first Ansatz for a circle statistic S_{ij} to measure the match between circles i, j would be the convolution of the temperature fluctuations along two circles. As discussed
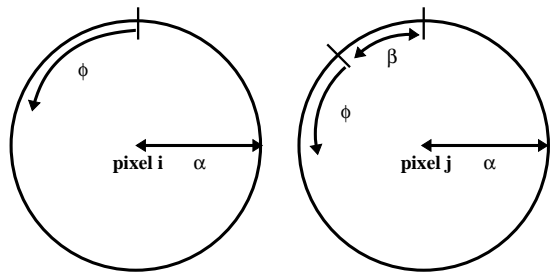
‾‾‾‾‾‾‾‾‾

[1] http://healpix.jpl.nasa.gov

FIG. 2: A circle of opening angle α centered at pixel i, and a circle centered at pixel i with its phase shifted by β.

in [6], this would lead to a dominance of long wavelength (small m) Fourier modes along the circles, making S_{ij} rather insensitive to small-scale fluctuations. To compensate for this, [1] introduced an additional factor of the wavenumber m in the convolution (this is equivalent to the usual factor of $\ell(\ell+1)$ used to scale the two dimensional power spectrum). Thus, in order to compare two circles of opening angle α centered around pixel numbers i and j, we employ the circle statistic

$$
\begin{aligned}
S_{ij}(\alpha, \beta) = {} & \frac{1}{\sum_{m=0}^{n/2} m \left(|T_{im}(\alpha)|^2 + |T_{jm}(\alpha)|^2 \right)} \\
& \times \Bigg(\sum_{m=0}^{n/2} m T_{im}^*(\alpha) T_{jm}(\alpha) e^{-\frac{2\pi i m \beta}{n}} \\
& + \sum_{m=0}^{n/2} (n-m) T_{im}^*(\alpha) T_{jm}(\alpha) e^{-\frac{2\pi i m \beta}{n}} \Bigg), \quad (1)
\end{aligned}
$$

where β is the relative phase between the two circles and $T_{im}(\alpha)$ is the Fourier transform of the temperature fluctuation $\frac{\Delta T}{T}$ around circle i

$$
\frac{\Delta T}{T}(i, \phi) = \sum_{m=0}^{n-1} T_{im} e^{\frac{2\pi i m \phi}{n}}, \quad (2)
$$

where $n = 512$ along the circle (see Figure 2). For a search for orientable manifolds, we replace all occurrences of $T_{im}^*(\alpha)$ in the numerator by $T_{im}(\alpha)$. Notice that we use the conventions of the libfftw package[23][2]: positive frequencies are stored in the first half of the array $T_{im}, m = 0 \ldots \frac{n}{2}$, and negative frequencies are stored in backwards order from the end of the array, making $T_{im} = T_{i(n-m)}^*$[3]. We then use as statistic the maximum of $S_{ik}(\alpha, \beta)$ over all relative phases β

$$
S_{ij}^{\max}(\alpha) \equiv \max_{\beta} S_{ij}(\alpha, \beta). \quad (3)
$$

‾‾‾‾‾‾‾‾‾

[2] http://www.fftw.org
[3] Using the real–to–complex and complex–to–real routines enables us to save the Fourier transforms for a single circle of a given opening angle in an complex array of length $\frac{n}{2}$ instead of n.
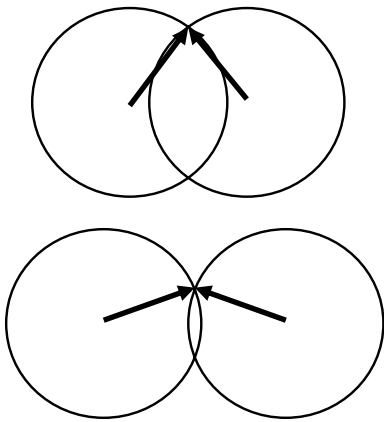
FIG. 3: Doppler contribution to the matching circle signal. Small circles (bottom) have opposite Doppler contributions, whereas large circles (top) obtain similar Doppler contributions. Thus large circles show a smaller deviation from $S_{ij}^{\mathrm{max}} = 1$.

For perfectly matching circles, $S_{ij}^{\mathrm{max}}(\alpha) = 1$, and for perfectly uncorrelated circles, $S_{ij}^{\mathrm{max}}(\alpha) \approx 0$. In practice, these ideal values are not realized due to noise contribution from several different effects. First of all, the Doppler effect at the surface of last scattering creates a different signal depending on the position of the observer, making larger matching circles closer to $S_{ij}^{\mathrm{max}} \approx 1$ whereas smaller circles will have $S_{ij}^{\mathrm{max}} < 1$ (see Figure 3). Another contribution comes from line–of–sight effects, especially the ISW effect, as the CMB photons from different directions traverse through different patches of space. The combination of these effects reduces the signal in S_{ij}^{max}, making potential matching circles less than perfect (see Figure 1 in [1]).

For this analysis, we used the WMAP7 temperature maps [24]. Outside the WMAP Kp12[4] sky mask, we used the same template cleaning method as [25]. Inside the Kp12 sky cut, we used the WMAP ILC map[5]. While this choice implied that the noise properties and resolution of the map differed between the two regions, the effect on the circle search was relatively small as the ILC map was only used for 5.8% of the pixels.

In order to estimate the significance of potential spikes in the statistics, we created approximate random realizations of the CMB[6]. To this end, we compute the $a_{\ell m}$'s of the cleaned CMB map. Then, we scramble them by randomly interchanging the m index for fixed ℓ's, and compute a "random" CMB map from the scram-

---

[4] http://lambda.gsfc.nasa.gov/product/map/dr1/intensity_mask.cfm
[5] http://lambda.gsfc.nasa.gov/product/map/dr4/ilc_map_get.cfm
[6] In contrast to the WMAP 1 year data that was examined in [1], here the statistics is not noise-dominated. In particular this means that the estimator for the false detection rate devised in [1] is not applicable for the WMAP7 year data.
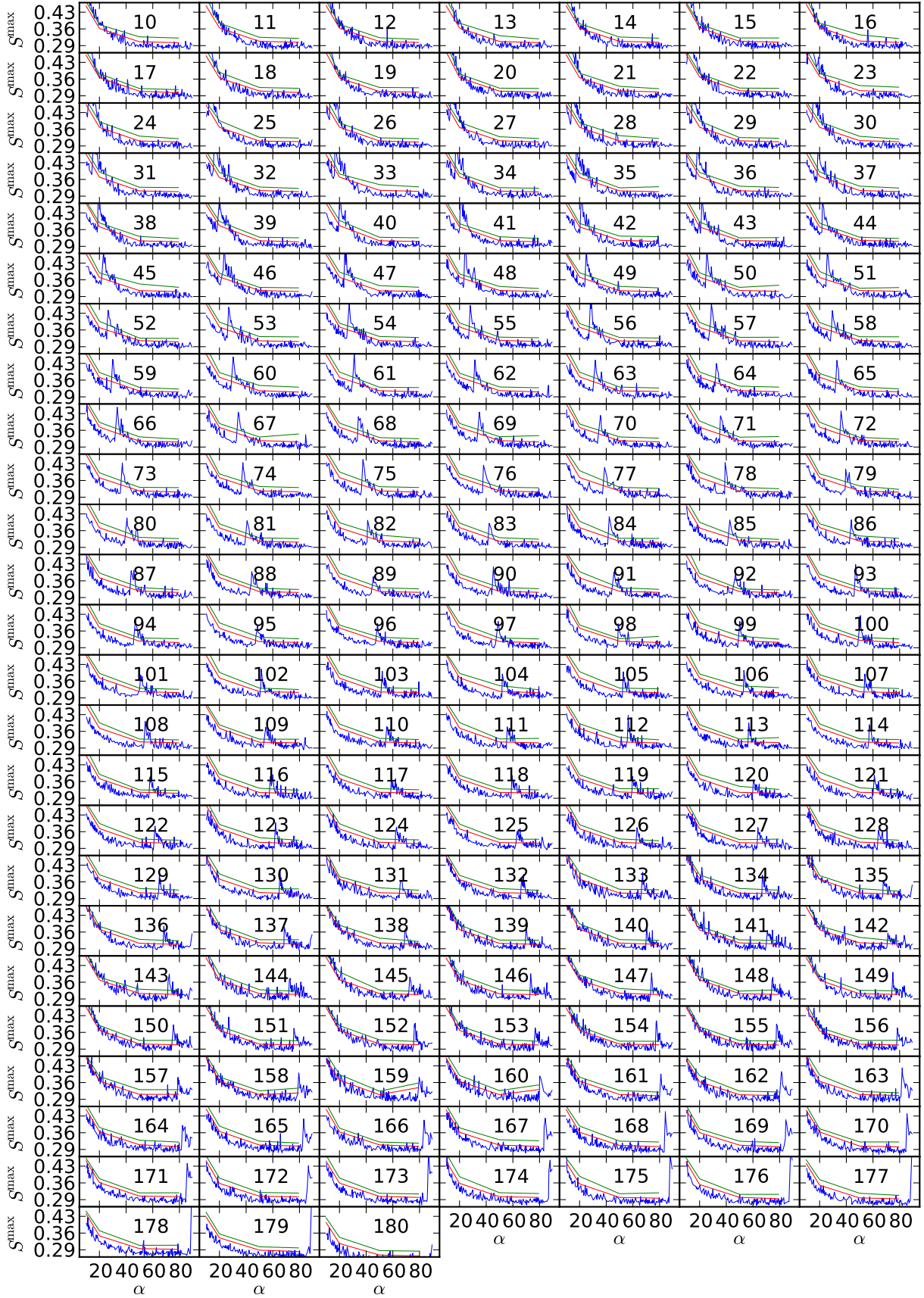
bled $a_{\ell m}$'s. Using this map, we compute the statistics for matching (non-)orientable circle pairs for opening angles $\alpha = 20°, 50°, 80°$ and all integer separation angles θ. Repeating this 1000 times, we obtain an estimate of the probability density function (pdf) of S^{max}. While there are enough samples to give a reliable estimate of the 95.4% (2σ) confidence level (CL), the quoted 99.7% (3σ) CL is at most a rough estimate. If the sky noise were isotropic, then this randomization process would generate simulated maps with the same statistical properties as the WMAP observations. However, because of anisotropies due to spatial variations in the WMAP noise (which is larger near the ecliptic plane) and variations in the resolution of our map (due to the need to use the ILC map in the galactic plane), these simulated maps only approximate the WMAP sky maps.

III. RESULTS

Implementing the procedure outlined in the previous section, we present the results of the searches and describe the systematic effects we encountered, both for orientable and non-orientable topologies.

Apart from a possible signal, there are simple random statistical fluctuations which are expected to exceed the 95% CL. To estimate the number of random fluctuations, we note that this can be viewed as a series of Bernoulli trials with probability $p = 0.05$ for success, i.e. for a spike above 95% CL. Per separation angle θ, we probed $n = 190$ values of the opening angle α (by choosing it to lie on a grid deriving from the position of the rings in the Healpix scheme for $n_{\mathrm{side}} = 128$. The probability distribution function for having i excursions above the $2\sigma/95.4\%$ CL for a sequence of n Bernoulli trials is given by the Binomial distribution

$$p^i (1-p)^{n-i} \binom{n}{i} , \qquad (4)$$

whose expectation value is given by

$$\langle N \rangle = \sum_{i=1}^{n} i p^i (1-p)^{n-i} \binom{n}{i} = np = 8.7 . \qquad (5)$$

Thus, we expect about 9 spikes above the 2σ CL per separation angle θ. Similarly, we expect about 0.6 spikes above the 3σ CL per separation angle θ.

A. Search for Orientable Topologies

Searching for orientable topologies, we find spikes in the distribution of the statistics S as a function of opening angle α and separation angle θ (see Figure 4). The red (green) line indicate the $2\sigma(3\sigma)$ CL as determined from scrambling the $a_{\ell m}$'s which we described above.

FIG. 4: Searching for orientable topologies: The statistics S (solid blue line) as defined in Equation 1 as a function of opening angle α and separation angle θ (indicated by the numbers in the center of each plot). The red/ green line correspond to the $2\sigma/3\sigma$ CL. The spikes come from circles osculating at the galactic anti-center and at $l = 109.44°$, $b = 27.8°$ (see Figure 7). Removing circles that touch these regions removes all features (see Figure 8).

FIG. 5: Searching for orientable topologies: For separation angle $\theta = 50°$, a plot of the statistics S as a function of opening angle α. Without cutting anything, the dashed black line shows an extended feature at $\alpha = \frac{1}{2}\theta = 25°$. Ignoring all circle pairs that overlap within $2.5°$ degrees of the galactic anti-center (GAC), the feature mostly disappears (solid blue line). The red (green) solid lines show the 95.4% (99.7%) CL on S, obtained by scrambling the $a_{\ell m}$ (see the main text). See Figure 7 for an explanation of the systematic spikes in S as well as Figure 8 for the final result after excising the offending circles.
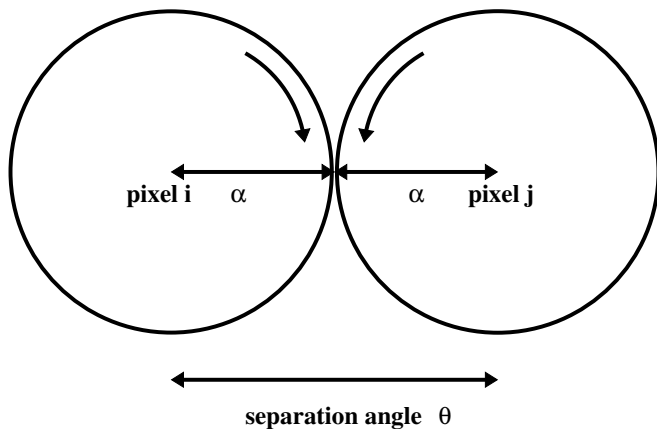

FIG. 6: As soon as the separation angle θ between the two circles becomes approximately twice their opening angle α, $\theta < 2\alpha$, the circles start partially overlapping, creating matching patterns in the statistics S^{max} as for orientable manifolds, the "kissing" segments match.

There is an extended feature whose position (as a function of the opening angle α) is correlated with the separation angle θ – it seems to be located at $\alpha = \frac{1}{2}\theta$. Figure 5 shows the values of S^{max} as a function of α for two circles separated by $\theta = 50°$, with a bump clearly visible around $\alpha = 25°$. This can be understood as the effect of two circles partially overlapping (see Figure 6). If two circles are separated by twice their opening angle α they osculate

("kiss"). For orientable manifolds this means that their patterns nearly match up along a segment. This effect is almost independent of the absolute magnitude of the opening angle α: the fraction of the circles that "kiss" is independent of α (up to effects of finite pixel size). However, it is interesting to note that most of the osculating circles that give the maximal S for a given separation angle and opening angle osculate at either of two positions: at the galactic anti-center, or at $l = 109.44°$, $b = 27.8°$ (see Figure 7).

Note that there is no known topology which would lead to such such a structure of spikes in the S statistics, correlating the opening angle with the separation angle, confined to just two positions on the sky and appearing both in the search for orientable topologies as well as in the search for non-orientable topologies (see next Subsection). Hence it is justified to remove all circles that touch either the galactic anti-center or the position $l = 109.44°$, $b = 27.8°$. The existence of this anomaly near the galactic anti-center is perhaps not surprising. The anti-center is in the middle of the ILC portion of the map, and ILC pixels have much more correlated noise properties than the rest of the map. The second point is near the region where the noise properties of the maps are very non-uniform (see Figure 3 in [26]).

First excising circles that osculate at the galactic anti-center, Figure 7c), and then those that osculate at $l = 109.44°$, $b = 27.8°$, Figure 7d), removes most systematic spikes from the S statistics. The peaks that are left for separation angles $\theta > 170°$ and opening angle $\alpha \approx 90°$ are caused by the fact that circles with $\alpha = 90°$ have an angular diameter of $180°$. Thus, two such circles, when separated by $\theta \approx 180°$ will start overlapping, until for $\theta = 180°$, they coincide, independent of the topology of the universe.

Hence Figure 8 presents the final result of the search for orientable topologies. The number of spikes above the 2σ and 3σ thresholds are consistent with random fluctuations. This leads us to conclude that the data is consistent at 99.7% CL with the null hypothesis of no non-trivial, orientable topology.

B. Search for Non-Orientable Topologies

Performing the search for non-orientable topologies on the cleaned CMB map, we again find a multitude of excursions above the 3σ CL (see Figure 9). There, we plot in blue the statistics S as a function of opening angle α and separation angle θ (the former indicated by the numbers in the middle of each panel). The red (green) line is the $2\sigma(3\sigma)$ CL obtained by scrambling the $a_{\ell m}$'s as described above. In particular, for low values of the separation angle θ, the signal lies consistently above the 3σ CL. The source of these excursions are again circles which touch either of two distinct spots: the galactic anti-center and $l = 109.44°$, $b = 27.8°$ (see Figure 10a). Disregarding all circles that come within $2.5°$ of the galactic

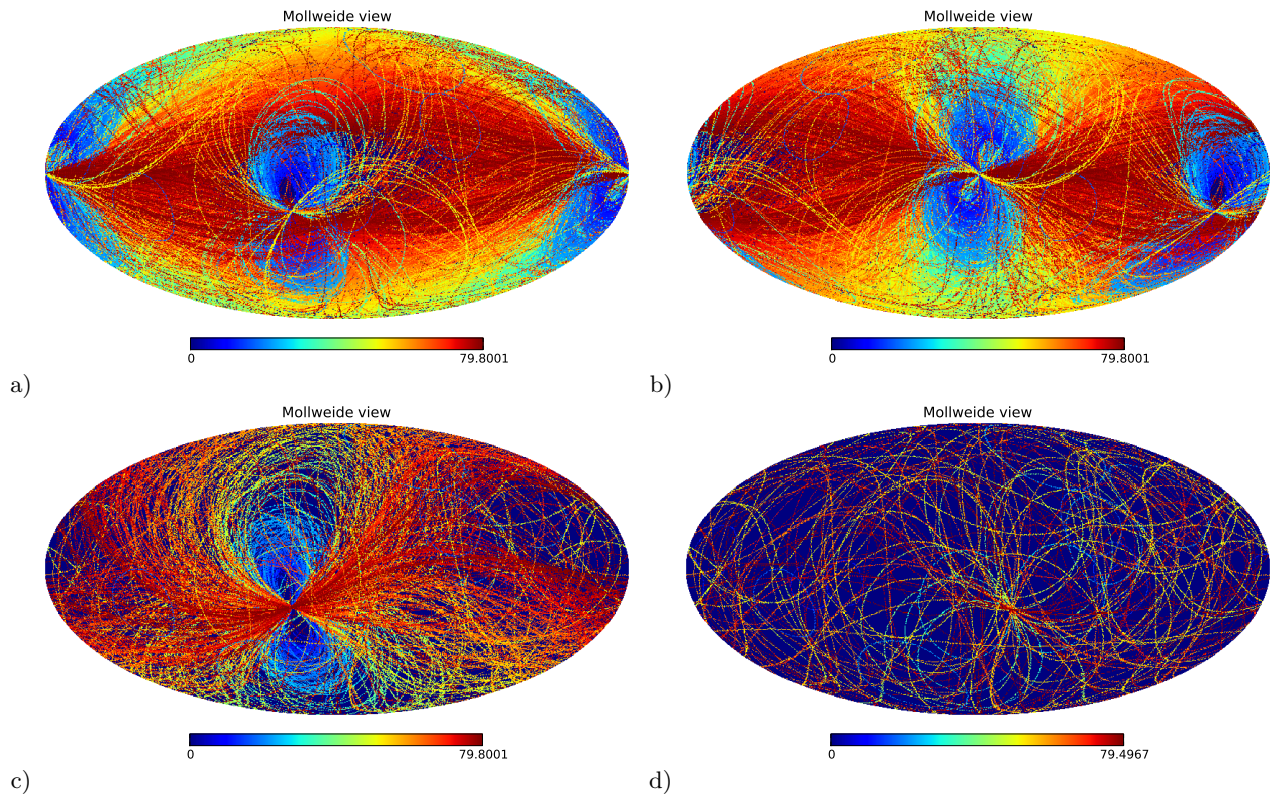FIG. 7: For the search for orientable manifolds: Location of the circles pairs with maximal statistics S that lies above the 3σ CL, colored by opening angle α. Note that the osculating circles at the galactic anti-center and at $l = 109.44°$, $b = 27.8°$ do not hint at a non-trivial topology. a) The highest signal comes from circle pairs osculating at the galactic anti-center and at $l = 109.44°$, $b = 27.8°$. b) same as a), but rotated by $180°$ such that the galactic anti-center is in the middle of the plot. c) Removing circle pairs that osculate at the galactic anti-center, the highest signal comes from pairs that osculate at $l = 109.44°$, $b = 27.8°$. d) Removing circles that osculate either at the galactic anti-center or at $l = 109.44°$, $b = 27.8°$, no special position on the sky is apparent.

anti-center, we still find many excursions above the 3σ CL (see Figure 10b). Finally, also removing circles that come within $2.5°$ of the position $l = 109.44°$, $b = 27.8°$, there is no structure left (see Figures 10c and 11).

Figure 11 presents the final, negative result of the search for a non-trivial, non-orientable topology of the universe. The remaining excursions above 2σ and 3σ are well explained by random statistical fluctuations as outlined in the previous subsection. This leads us to conclude that the data is consistent at 99.7% CL with the null hypothesis of no non-trivial, non-orientable topology.

IV. CONCLUSIONS AND OUTLOOK

We employed the circles-in-the-sky statistics first devised in [1], looking for pairs of matching circles of opening angles $10° < \alpha < 90°$ and separation angles $11° \le \theta \le 180°$. We positioned the circle centers on a grid with $N_{\text{side}} = 128$, but computed the statistics on the full $N_{\text{side}} = 512$ CMB map.

While the WMAP 7 year data brought quite some improvements in the noise of the $S_{ij}^{\max}$ statistics (c.f. Figure

2 in [1]), we find no hints of a non-trivial topology of the universe (see Figures 8 and 11). The new search covered a much wider range of possible topologies, and by extending the search to circles with opening angles as small as $10°$, we have extended the previous bound on the size of the Universe to 98.5% of the diameter of the last scattering surface, or approximately 26Gpc.

There are systematic effects coming from both members of a circle pair touching either the galactic anti-center or the position $l = 109.44°$, $b = 27.8°$ (see Figures 7 and 10). As these positions appear both when looking for orientable and non-orientable manifolds, they cannot be of topological origin, but point towards a contamination of the map at these positions. The galactic anti-center region contains significant amounts of galactic emission. While the ILC maps used in this analysis attempt to remove most of this emission, the correlated residuals are a likely source of contamination in the circle searches.

We are looking forward to the data release of the Planck mission, which will offer an exciting new, sharper view of the surface of last scattering, allowing for a better search of signs of non-trivial topology by removing noise
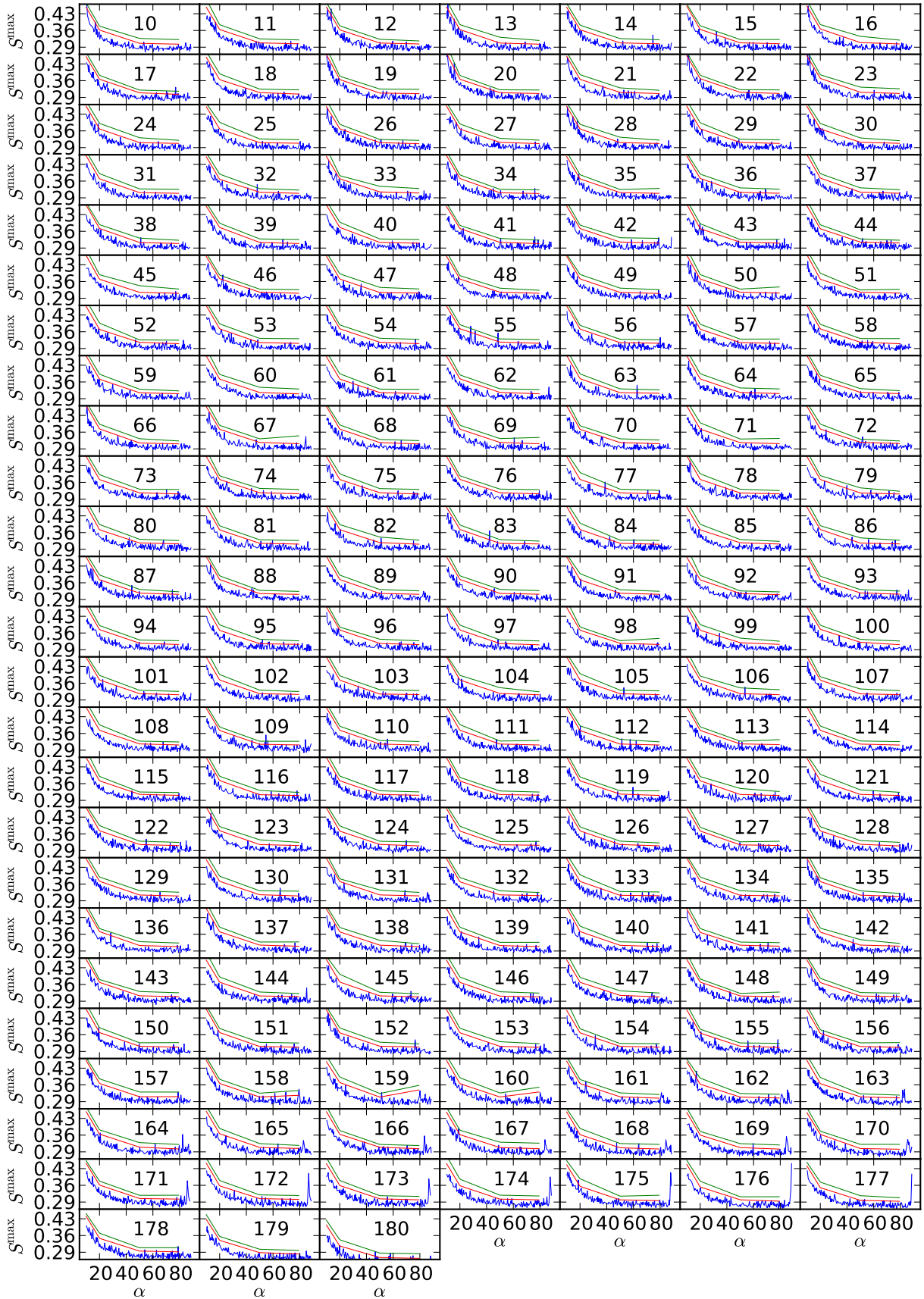
FIG. 8: Searching for orientable topologies, final result: The statistics S (solid blue line) as defined in Equation 1 as a function of opening angle α and separation angle θ (indicated by the numbers in the center of each plot). The red/ green line correspond to the 2σ/3σ CL. We disregard circles that touch either the galactic anti-center or $l = 109.44°$, $b = 27.8°$. The peaks for separation angles $\theta > 170°$ and opening angle $\alpha \approx 90°$ are caused by the fact that circles with $\alpha = 90°$ have an angular diameter of $180°$. Thus, two such circles, when separated by $\theta \approx 180°$ will start overlapping, until for $\theta = 180°$, they coincide, independent of the topology of the universe. No signs of a non-trivial orientable topology are found.
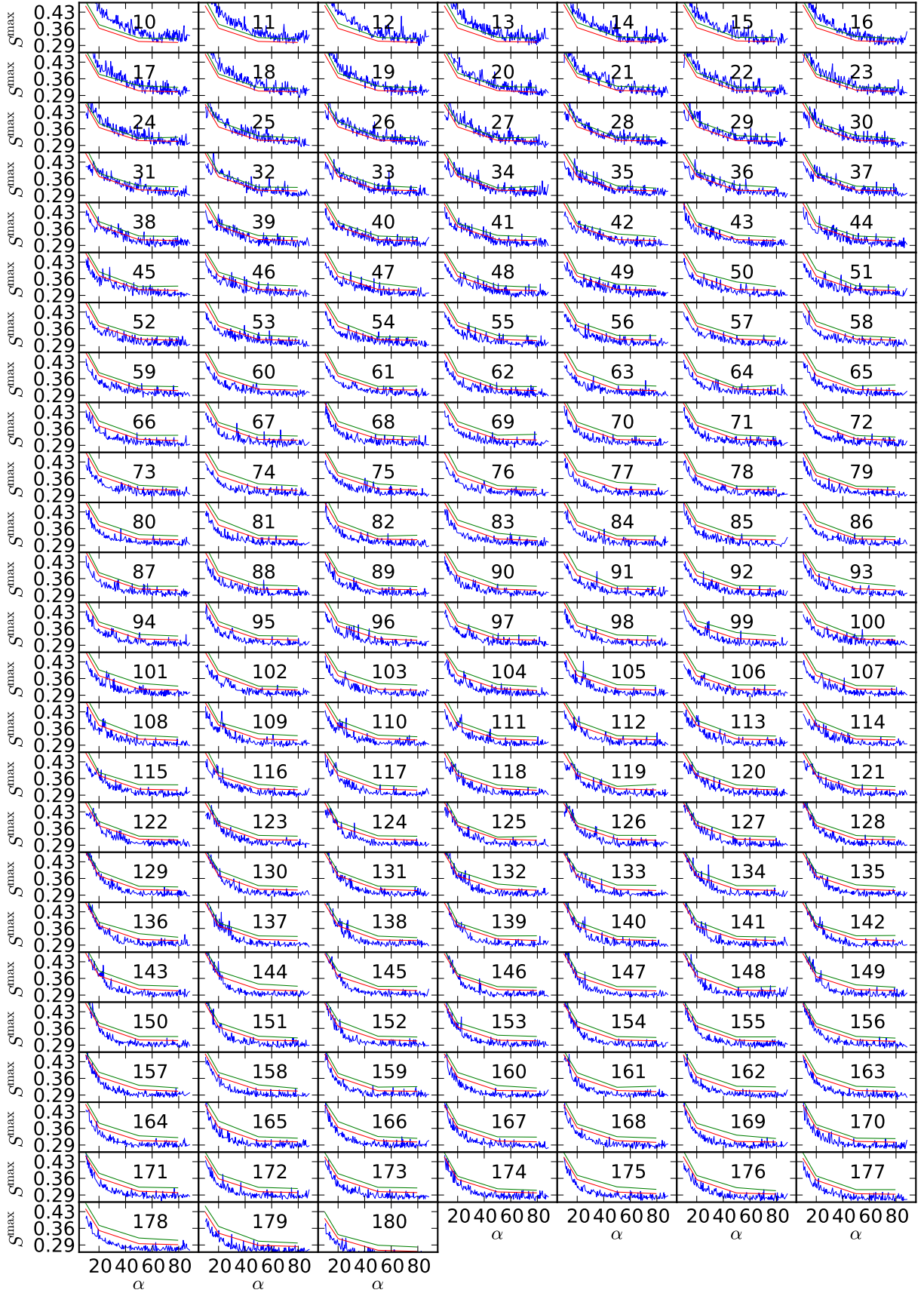
FIG. 9: Searching for non-orientable topologies: The statistics S (solid blue line) as defined in Equation 1 as a function of opening angle α and separation angle θ (indicated by the numbers in the center of each plot). The red/ green line correspond to the $2\sigma/3\sigma$ CL. The spikes come from circles osculating in the galactic anti-center and at $l = 109.44°$, $b = 27.8°$ (see Figure 10). Removing circles that touch these regions removes all features (see Figure 11).
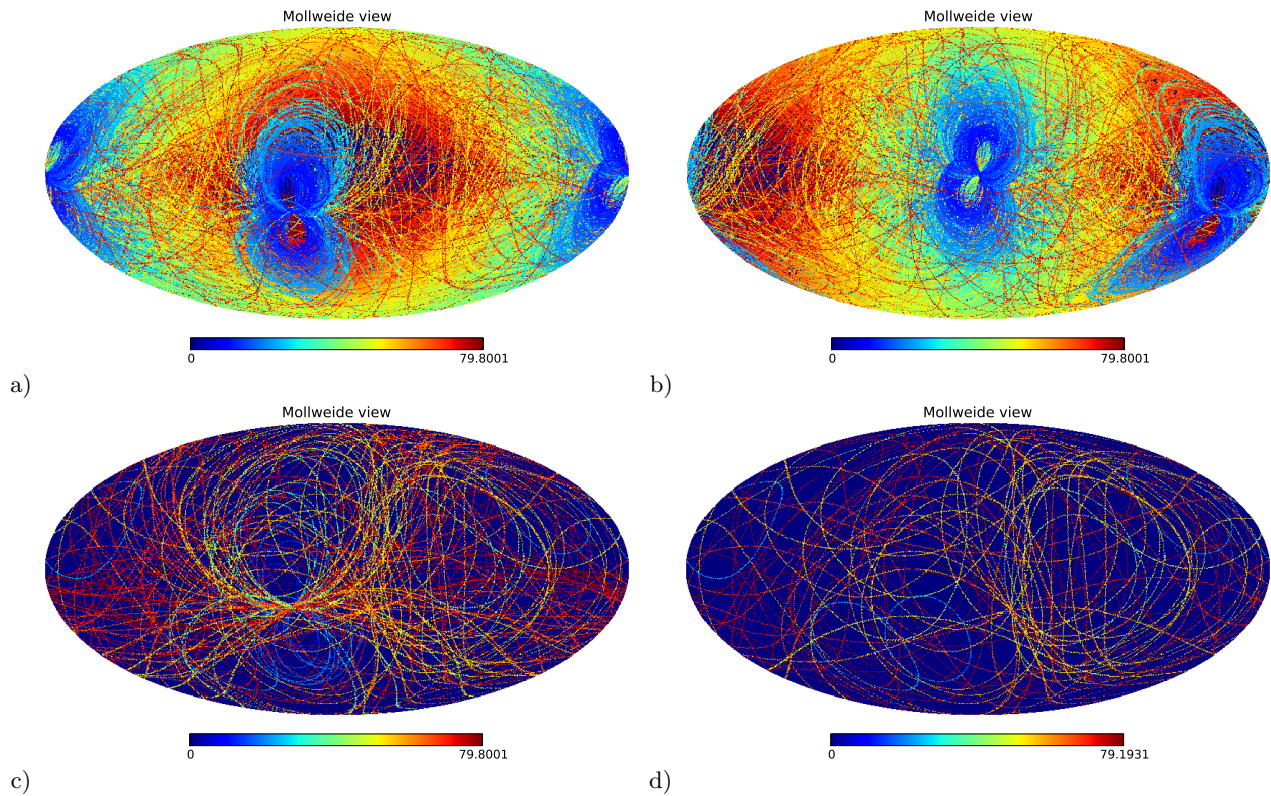
FIG. 10: For the search for non-orientable manifolds: Location of the circles pairs with maximal statistics S that lies above the 3σ CL, colored by opening angle α. Note that the circles that touch either the galactic anti-center or $l = 109.44°$, $b = 27.8°$ do not hint at a non-trivial topology. a) The highest signal comes from circle pairs osculating at the galactic anti-center and at $l = 109.44°$, $b = 27.8°$. b) same as a), but rotated by $180°$ such that the galactic anti-center is in the middle of the plot. c) Removing circle pairs that touch the galactic anti-center, the highest signal comes from pairs that touch $l = 109.44°$, $b = 27.8°$. d) Removing circles that touch either the galactic anti-center or $l = 109.44°$, $b = 27.8°$, no special position on the sky is apparent.

particularly at smaller separation angles $\alpha < 30°$. Further advances in computing power will enable a search on a full $N_{\text{side}} \geq 512$ grid of circle positions.

Acknowledgements

It is a pleasure to thank Jeff Weeks for interesting discussions. Some of the results in this paper have been derived using the HEALPix[27] package. This work made use of the High Performance Computing Resource in the Core Facility for Advanced Research Computing at Case Western Reserve University. We acknowledge the use of the Legacy Archive for Microwave Background Data

[1] Neil J. Cornish, David N. Spergel, Glenn D. Starkman, and Eiichiro Komatsu. Constraining the Topology of the Universe. *Phys. Rev. Lett.*, 92:201302, 2004.

[2] Neil J. Cornish, David N. Spergel, and Glenn D. Starkman. Circles in the Sky: Finding Topology with the Microwave Background Radiation. *Class. Quant. Grav.*, 15:2657–2670, 1998.

[3] Janna J. Levin. Topology and the cosmic microwave background. *Phys. Rept.*, 365:251–333, 2002.

[4] Neil J. Cornish, David Spergel, and Glenn Starkman. Can COBE see the shape of the universe? *Phys.Rev.*, D57:5982–5996, 1998.
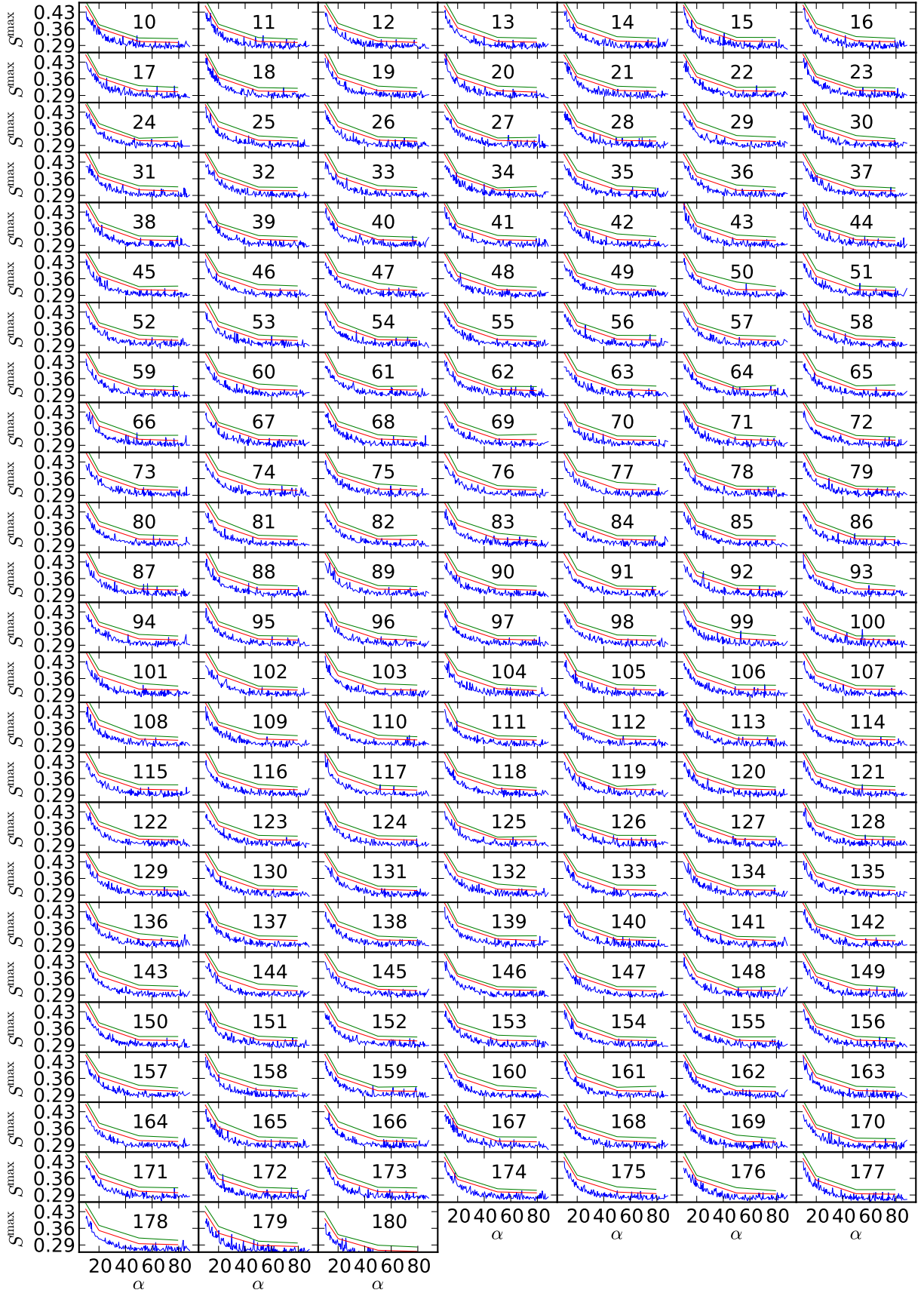
FIG. 11: Searching for non-orientable topologies, final result: The statistics S (solid blue line) as defined in Equation 1 as a function of opening angle α and separation angle θ (indicated by the numbers in the center of each plot). The red/ green line correspond to the $2\sigma/3\sigma$ CL. We disregard circles that touch either the galactic anti-center or $l = 109.44°$, $b = 27.8°$. No signs of a non-trivial non-orientable topology are found.

[5] Neil J. Cornish, David N. Spergel, and Glenn D. Starkman. Measuring the topology of the universe. *Proc.Nat.Acad.Sci.*, 95:82, 1998.

[6] Joey Shapiro Key, Neil J. Cornish, David N. Spergel, and Glenn D. Starkman. Extending the WMAP Bound on the Size of the Universe. *Phys. Rev.*, D75:084034, 2007.

[7] J. Richard Bond, Dmitry Pogosian, and Tarun Souradeep. Constraints on compact hyperbolic spaces from COBE. 1996.

[8] J. Richard Bond, Dmitri Pogosian, and Tarun Souradeep. Computing CMB anisotropy in compact hyperbolic spaces. *Class.Quant.Grav.*, 15:2671–2687, 1998.

[9] Tarun Souradeep, Dmitry Pogosian, and J. Richard Bond. Probing cosmic topology using CMB anisotropy. 1998.

[10] J. Richard Bond, Dmitry Pogosian, and Tarun Souradeep. CMB anisotropy in compact hyperbolic universes. 1. Computing correlation functions. *Phys.Rev.*, D62:043005, 2000.

[11] J. Richard Bond, Dmitry Pogosian, and Tarun Souradeep. CMB anisotropy in compact hyperbolic universes. 2. COBE maps and limits. *Phys.Rev.*, D62:043006, 2000.

[12] Marc Lachieze-Rey and Jean-Pierre Luminet. Cosmic topology. *Phys.Rept.*, 254:135–214, 1995.

[13] R. Lehoucq, M. Lachieze-Rey, and J.P. Luminet. Cosmic crystallography. *Astron.Astrophys.*, 313:339–346, 1996.

[14] Jean-Pierre Luminet and Boudewijn F. Roukema. Topology of the universe: Theory and observation. 1999.

[15] Jean-Philippe Uzan, Roland Lehoucq, and Jean-Pierre Luminet. New developments in the search for the topology of the universe. 1998.

[16] Jean-Philippe Uzan, Roland Lehoucq, and Jean-Pierre Luminet. A new crystallographic method for detecting space topology. *Astron.Astrophys.*, 351:766, 1999.

[17] Roland Lehoucq, Jean-Philippe Uzan, and Jean-Pierre Luminet. Limits of crystallographic methods for detecting space topology. *Astron.Astrophys.*, 363:1, 2000.

[18] Alain Riazuelo, Jeffrey Weeks, Jean-Philippe Uzan, Roland Lehoucq, and Jean-Pierre Luminet. Cosmic microwave background anisotropies in multi-connected flat spaces. *Phys.Rev.*, D69:103518, 2004.

[19] Jeffrey Weeks, Jean-Pierre Luminet, Alain Riazuelo, and Roland Lehoucq. Well- proportioned universes suppress CMB quadrupole. *Mon.Not.Roy.Astron.Soc.*, 352:258, 2004.

[20] Alain Riazuelo, Samuel Caillerie, Marc Lachieze-Rey, Roland Lehoucq, and Jean-Pierre Luminet. Constraining cosmic topology with cmb polarization. *Phys.Rev.D*, 2006.

[21] Anastasia Niarchou and Andrew H. Jaffe. Predicting and analyzing topological correlations in the cmb. *AIP Conf.Proc.*, 848:774–778, 2006.

[22] Anastasia Niarchou and Andrew Jaffe. Imprints of spherical non-trivial topologies on the CMB. *Phys.Rev.Lett.*, 99:081302, 2007.

[23] Matteo Frigo and Steven G. Johnson. The design and implementation of fftw3. *Proc. IEEE*, 93 (2):216231, 2005.

[24] N. Jarosik, C.L. Bennett, J. Dunkley, B. Gold, M.R. Greason, et al. Seven-Year Wilkinson Microwave Anisotropy Probe (WMAP) Observations: Sky Maps, Systematic Errors, and Basic Results. *Astrophys.J.Suppl.*, 192:14, 2011.

[25] B. Gold, N. Odegard, J.L. Weiland, R.S. Hill, A. Kogut, et al. Seven-Year Wilkinson Microwave Anisotropy Probe (WMAP) Observations: Galactic Foreground Emission. *Astrophys.J.Suppl.*, 192:15, 2011.

[26] C.L. Bennett et al. First year Wilkinson Microwave Anisotropy Probe (WMAP) observations: Preliminary maps and basic results. *Astrophys.J.Suppl.*, 148:1, 2003.

[27] K.M. Gorski, Eric Hivon, A.J. Banday, B.D. Wandelt, F.K. Hansen, et al. HEALPix - A Framework for high resolution discretization, and fast analysis of data distributed on the sphere. *Astrophys.J.*, 622:759–771, 2005.